Converting a Switching Solenoid to a Proportional Actuator

M.F. Rahman, N.C. Cheung, K.W. Lim

School of Electrical Engineering, University of New South Wales,
P.O. Box 1, Kensington, NSW 2052, AUSTRALIA.
Fax: ++612-662-2087 Email: f.rahman@unsw.edu.au

Abstract - Solenoids are presently used as cheap and robust switching components. These are variable reluctance devices with their characteristics dictated by a highly nonlinear magnetic circuit. This paper describes the development work done on converting a switching solenoid into a proportional device. It first investigates the magnetic characteristics of a solenoid, followed by developing a control model for the device. Based on this model, a dual rate cascade control scheme with a nonlinear force mapper is proposed for proportional control. This scheme is tested out by simulation and implemented on a Digital Signal Processor based control hardware.

1. Introduction

Solenoids are presently used as mechanical switching components only. They are simple in construction, rugged, relatively cheap to produce, and can be totally enclosed and sealed quite easily. However, these are not suitable for use in proportional control, largely due to the nonlinearity of their magnetic circuit and force equations.

Figure 1. shows the typical construction of a linear and limited travel solenoid valve. The total travel of such a solenoid is very short: in most cases it is less than one centimetre.

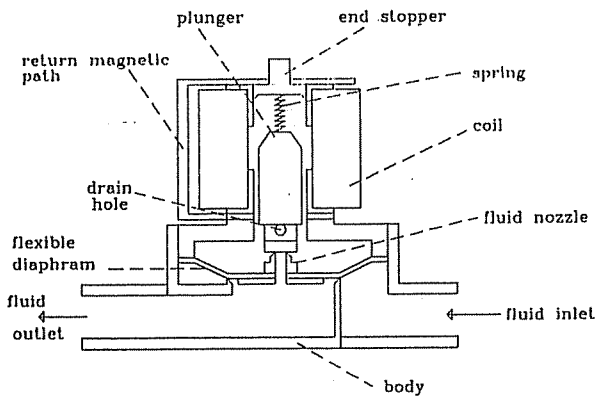

Figure 1 Construction of a solenoid valve

Present proportional actuators employ moving coil techniques working under constant magnetic field. This arrangement decouples the control from the nonlinear magnetic behaviour. On the other hand, solenoids are variable reluctance devices with their characteristics dictated by highly nonlinear magnetic circuit [1,2]. Therefore it is very difficult to operate a solenoid as a proportional actuator using traditional feedback techniques.

This paper describes the development and experimental work done on converting a solenoid into a proportional actuator. Section 2 examines the magnetic and control characteristics of a solenoid. A control model, including nonlinear magnetic characteristics is developed. Section 3 describes the dual rate cascade control strategy, and its mechanism of nonlinear magnetic characteristics compensation. Finally, section 4 reports the simulation and hardware implementation results of such a controller on switching industrial solenoid.

2. Development of the Control Model

Before any form of control strategy is proposed, a full control model of the solenoid need to be developed. Solenoid is a variable reluctance device with its force derived from the change of magnetic flux linkage. Therefore, the flux linkage relationships with current and position form the bases of the full control model [3,4,5].

2.1 Dynamic Characteristics of a Solenoid

A solenoid has a resistive and inductive circuit. Its voltage equation can be expressed as:

$$V = Ri + \frac{d\lambda}{dt} \tag{1}$$

where V is the terminal voltage and R is the resistance of coil. The flux linkage λ is a variable dependent on the current of the coil i and the air gap distance x. Therefore the voltage equation can be rewritten as:

$$V = Ri + (L_e + \frac{\partial\lambda(x,i)}{\partial i}) \cdot \frac{di}{dt} + \frac{\partial\lambda(x,i)}{\partial x} \cdot \frac{dx}{dt} \tag{2}$$

L_e is the inductance of the external circuit. Of the three terms in the equation (2), the first term is the resistive voltage drop. The second term is the inductive voltage due to change of current. The third term is known as `back e.m.f.' or `motional e.m.f'. and is caused by the motion of the plunger. Equation (2) can only be

solved if the magnetic characteristics of the solenoid are known.

On the mechanical side, the solenoid can be represented by a mass spring system:

$$m_p\ddot{x} = F_{mag} - K_s x - m_p g \tag{3}$$

where m_p is the mass of the plunger, K_S is the spring constant, g is the gravitational constant and F_{mag} is the force produced by magnetic field when the coil is energised. F_{mag} can be calculated from the co-energy W'. The co-energy can be estimated from the integration of flux linkage against current:

$$F_{mag} = \frac{\partial W'(x,i)}{\partial x} \tag{4}$$

$$W'(x,i) = \int_0^i \lambda(x,i)\cdot di \tag{5}$$

Since the variables i and x are fully independent and separable in relation to $\lambda(x,i)$, it is permissible to 'differentiate under the integral sign'. Equation (4) and (5) becomes:

$$F_{mag} = \int_0^i \left.\frac{\partial \lambda(x,i)}{\partial x}\right|_{i=const} \cdot di \tag{6}$$

For instantaneous value of F_{mag}, when x does not change during that short period of time, equation (6) can be written as:

$$F_{mag} = \frac{\partial \lambda(x,i)}{\partial x}\cdot i \tag{7}$$

From equations (2), (3), and (7) we can write a non linear state model:

$$\frac{dx}{dt} = v \tag{8}$$

$$\frac{dv}{dt} = \left(\frac{\partial \lambda(x,i)}{\partial x}\cdot i - K_s x - m_p g\right)\cdot\frac{1}{m_p} \tag{9}$$

$$\frac{di}{dt} = \left(V - Ri - \frac{\partial \lambda(x,i)}{\partial x}\cdot\frac{dx}{dt}\right)\cdot\frac{1}{L_e + \frac{\partial \lambda(x,i)}{\partial i}} \tag{10}$$

In equations (8) to (10), $\frac{\partial \lambda}{\partial x}$ and $\frac{\partial \lambda}{\partial i}$ are obtained from a model of the magnetic characteristics. Flux linkage relationships with current and position needs to be found to complete the state model.

2.2 Measurement of Flux

Many methods are available on measuring the magnetic characteristics of switched reluctance motors [11] [12], This paper uses a measurement technique based on a.c. excitation and induced e.m.f. measured by a search coil wound on the solenoid's plunger [1]. The plunger is also slightly modified to accommodate a non ferric screw for accurate positioning during measurement.

To measure the induced flux, an a.c. voltage is fed into the solenoid coil, with the plunger fixed at a predetermined position. Voltage and current waveforms are digitised and recorded into the computer at 5kHz per channel (100 sampling points per a.c. cycle). This procedure is repeated again with plunger positions incremented at 0.5mm interview. The whole process is completed when all the plunger positions' voltage and current waveforms have been measured. The measurement set up is shown in figure 2.

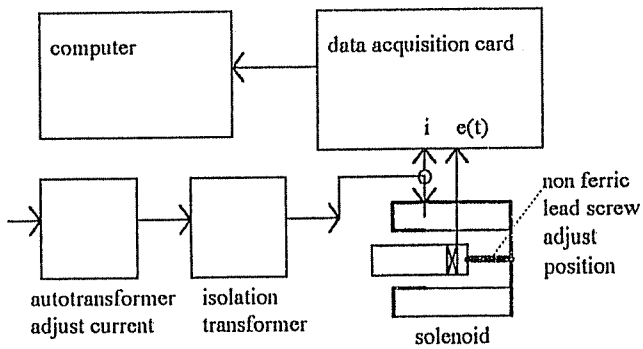

Figure 2 Measurement of magnetic characteristic

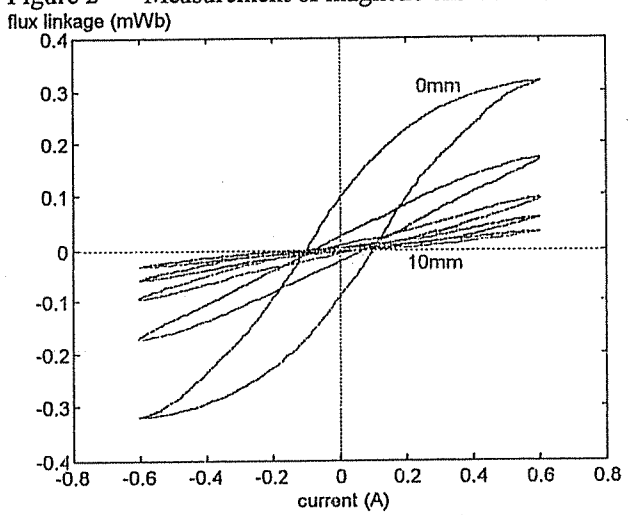

Figure 3 Hysteresis loops at different positions

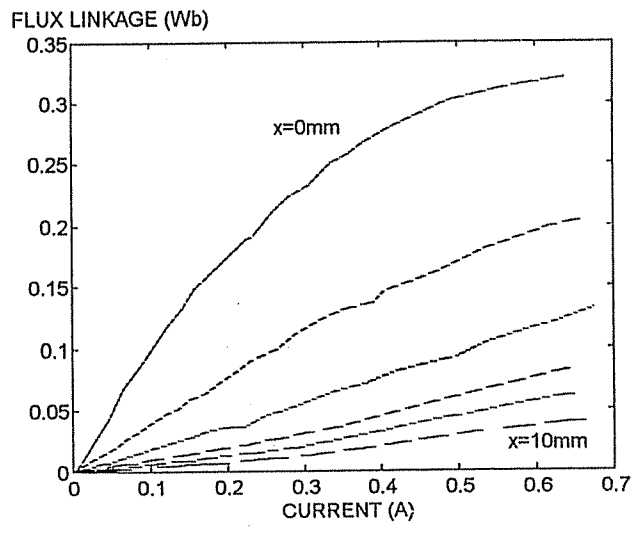

Figure 4 Flux linkage versus current

Flux and flux linkage through the plunger can be obtained by the following equations:

$$\Phi(t) = -\frac{1}{N_s}\int_0^t e(t)\cdot dt \qquad (11)$$

$$\lambda(t) = N\cdot\Phi(t) \qquad (12)$$

where $\Phi(t)$ is the flux, $\lambda(t)$ is the flux linkage, $e(t)$ is the voltage output from the search coil, N is the number of turns of the solenoid coil, and N_S is the number of turns of the search coil. Figure 3 shows the hysteresis loops at different plunger positions obtained from this measurement method.

By joining the vertex of the hysteresis loops, the magnetic characteristics of flux linkage versus current at different positions (figure 4), and the flux linkage versus position at different current levels can be obtained (figure 5).

Change of flux linkage creates force on the plunger, as described in equation (7). Therefore force is also a two dimensional relation with current and position as shown in figure 6. The plot is obtained by actual measurement of static force against position and current. Alternatively, the force function can be calculated by applying equation (7) to the graphic plot of figure 5.

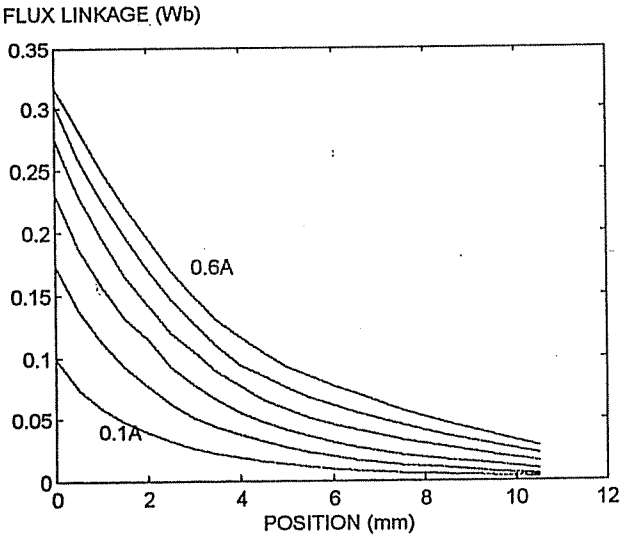

Figure 5 Flux linkage versus position

3. The Proportional Actuator

There is little in recent literature which deals with proportional control of solenoids. For the related problem of rotary switched reluctance motors, M. Illic-Spong et al [7,8] used Feedback linearizing technique to tackle the problems of nonlinearity. Though it has produced promising results in simulation, the method is too complicated to implement in real time. D.G. Taylor [9] used reduced order composite control for the variable reluctance motor, however, external analogue hardware is required to linearise the current voltage relation of the switched reluctance motor.

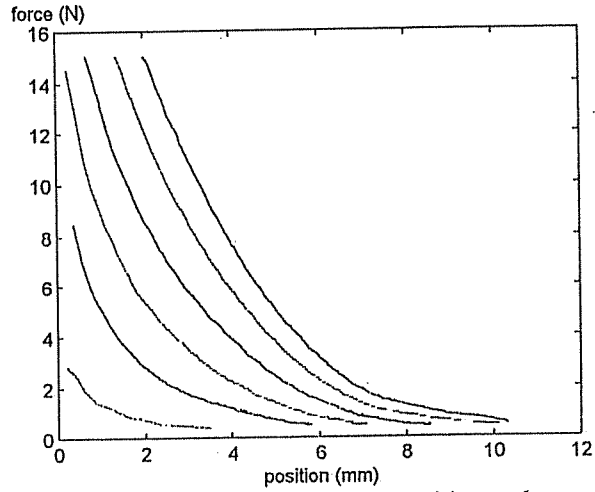

Figure 6 Variation of force against position and current

Exploiting the fact that the current dynamics is at least an order faster than the mechanical dynamics, this paper proposes a dual rate cascade control approach. A fast inner loop current controller is employed to regulate the current-voltage nonlinearities of the solenoid, while a slower outer loop trajectory controller is used to control the mechanical dynamics. On top of this, a nonlinear function is included to compensate the nonlinearities of force against current and position. Figure 7 is the overall block diagram of the control system.

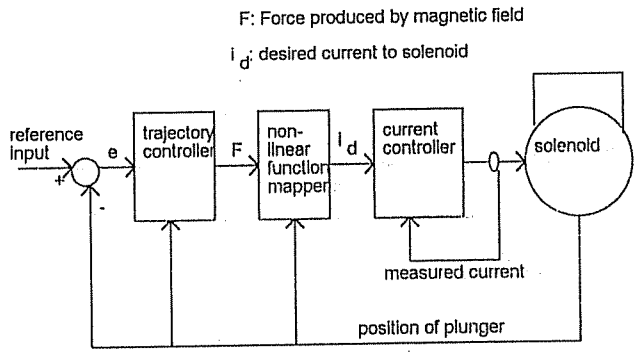

Figure 7 Block diagram of the control system

3.1 The Current Controller

A current controller is employed to linearise the current-voltage relation of the solenoid. A simple PI controller is proposed.

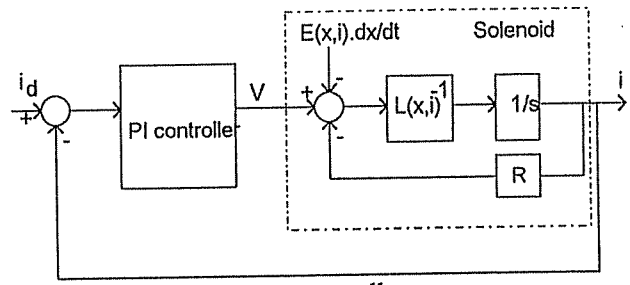

Figure 8 The current controller

Position can be assumed to be stationary during the control time frame of the current controller, since current

dynamics are much faster than mechanical dynamics. Thus, equation (2) can be simplified to:

$$V = Ri + L(i)\frac{di}{dt} + E(i)\frac{dx}{dt} \qquad (13)$$

where $L(i) = L_e + \frac{\partial \lambda}{\partial i}$ and $E(i) = \frac{\partial \lambda}{\partial x}$. $E(i)$ constitutes a disturbance term to the current controller as shown in figure 8. However, under normal operation, $E(i)$ constitutes less than 5% disturbance to the overall equation. Moreover, $E(i)$ is approximately constant over operation range of i, as shown in figure 5. Also, figure 4 shows that $L(i)$ is also approximately constant within the operating range, except when $x=0$. Thus, a PI controller is sufficient to control a solenoid which essentially has a resistive-inductive loading.

Standard Ziegler Nichols procedure can be used to tune the controller. Since the controller is least stable when inductance is large, the current controller should be tuned at x=0, when the inductance is at its largest.

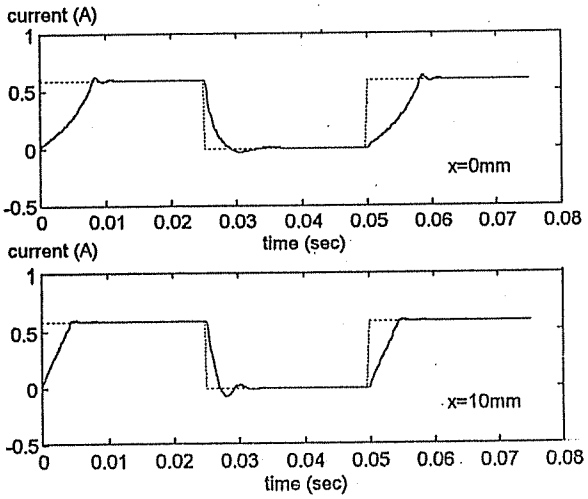

Figure 9 Response of the current controller with anti-windup .

Solenoids have large inductance; to avoid excessive saturation to the integrator during step inputs, anti-windup features should be present in the controller.

Figure 9 is the dynamic response of the current controller. The worst case step response time is less then 0.01sec.

3.2 The Nonlinear Function Mapper for Force Control

The nonlinear function bridges the link between the trajectory controller and the current controller. It receives force requirements from the trajectory controller and outputs desired current set points to the current controller. Since the relations of force, current, and position are nonlinear in nature, a lookup table is used to translate the force and position inputs to desired current outputs.

Figure 10 is the force profile of the solenoid, this information is stored as a two dimensional look up table. A 20x20 elements look up table with two dimensional linear interpolation is sufficient to describe the force profile with an accuracy of ±5% [10].

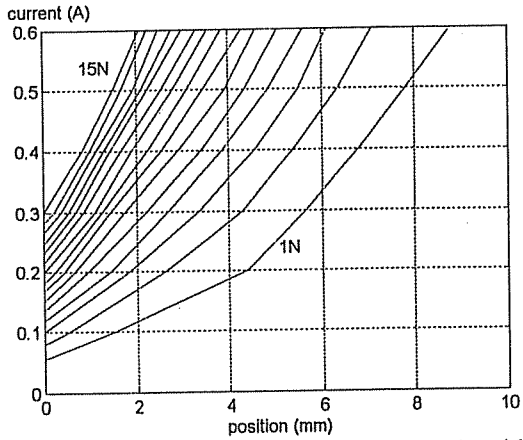

Figure 10 Measured force profile of the solenoid

3.3 The Trajectory Controller

The trajectory controller forms the essential part of the slow sub-system. It is a typical PID controller. The controller's operation is based on the assumption that the current controller has perfect tracking capability, and the non linear function mapper generates the linearised current command i_d to the current controller. Equation (7) is rearranged to form the mechanical equation:

$$F = m_p \cdot \frac{dv}{dt} + Ks \cdot x + m_p \cdot g \qquad (14)$$

The required force is calculated from the plunger's position x, and acceleration dv/dt. The acceleration value, derived from the output of the PID controller, is fed into equation (14) to calculate the required force F.

4. Implementation and Results

A typical industrial switching solenoid valve is employed to implement the proportional actuator. This type of solenoid is being used in many types of industrial applications. Its construction is shown in figure 1. The solenoid has the following specifications:

Make	Goyen Controls
Type	Two stage switching solenoid valve
Stroke length	10mm
Operating voltage	24V d.c.
Maximum current	0.6A
Resistance	40ohms
Inductance	0.35-1.1H
No of turns of coil	2240

4.1 Simulation of the Controller

The control system including full model of the solenoid is simulated to find out the performance of the

system. Figure 11 is the block diagram for the simulation.

Results of the simulated trajectory response and step response of the controller is shown in figure 13.

4.2 Hardware Setup

A Digital Signal Processor is used to implement the controller in hardware. A half bridge power MOSFET drivers with ±65V supplies are used in the output stage. The outer loop samples at 1kHz, while the inner loop samples at 4kHz. PWM chopping frequency is set to 12.5kHz. The hardware setup is shown in figure 12.

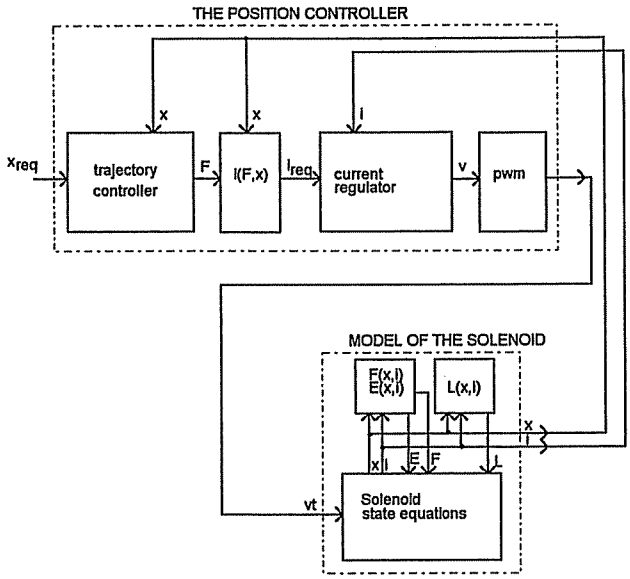

Figure 11 Simulation of the controller

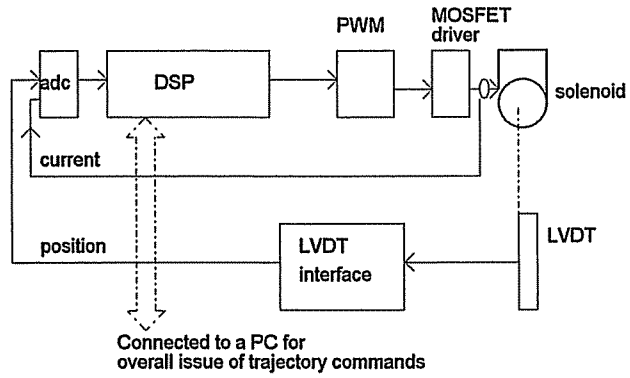

Figure 12 Setup of the control system

4.3 Results

Figure 13 shows the simulated step response and trajectory tracking response of the proportional solenoid. The simulated results show that the controller can control the plunger with reasonably high accuracy, speed and stability.

These results are very similar to the results obtained from hardware implementation, which are shown in figure 14. This confirms that the solenoid's model is valid and is sufficiently accurate.

The trajectory response of figure 14b shows that the response is more oscillatory when the air gap is small. This is partially due to the hysteresis effect and the increase of inductance, which tends to make the control system less stable. It is also caused by the bulging of the spring, which creates additional friction to the travel of the plunger. Therefore it is best to avoid the 0-1.5mm operating region.

The other end of the operating region is also difficult. Figure 10 shows that the inward force produced can never be greater than 1N when plunger is at 9mm. The outward force produced by the spring is also very weak, since the spring is nearly fully extended at this position. The operational force range is very limited around this region. Therefore it is also best to avoid the 8.5-10mm operating region.

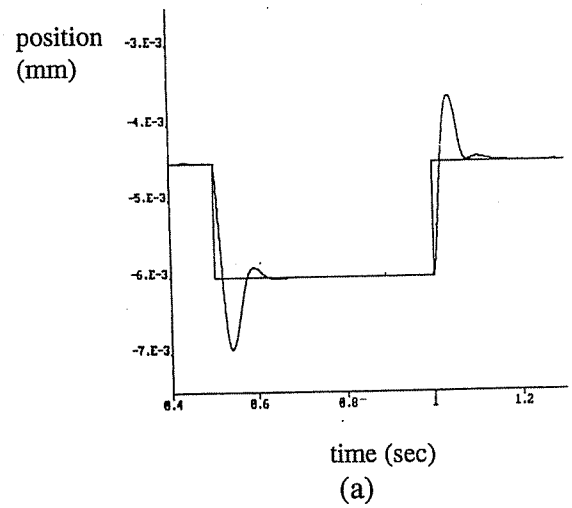

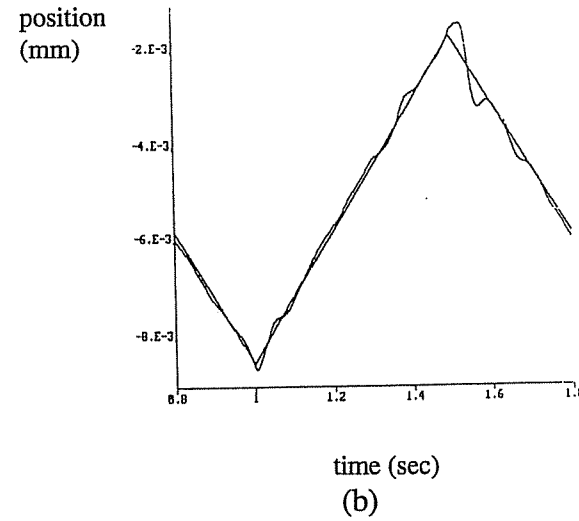

Figure 13 Simulated responses of the controller: (a) step response, (b) trajectory following

To conclude, the operating range of the solenoid should be limited to 1.5-8.5mm for the chosen solenoid. Figure 15 shows the stiffness of the control system. The restoring force acting on the plunger is measured when the plunger is deviated from its original set point position of 5mm. There is a large force change around the ± 0.1mm region, then the force change becomes more

gentle outside this region. Overall the reasonably high stiffness of the system indicates that the system can be controlled to a high degree of accuracy.

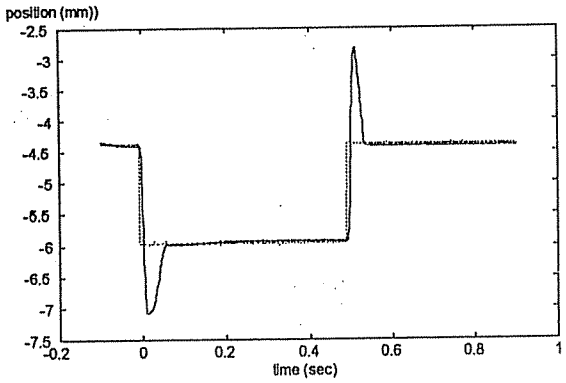

(a)

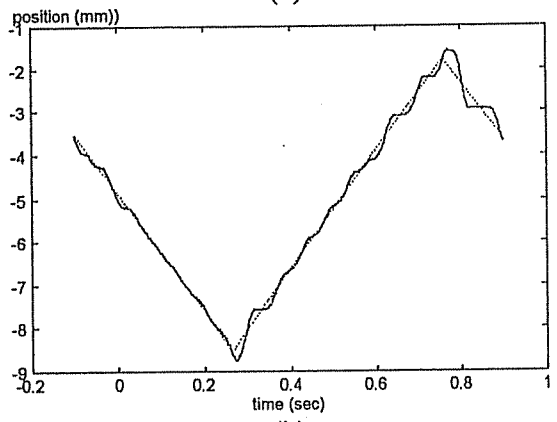

(b)

Figure 14 Experimental responses of the controller: (a) step response, (b) trajectory following

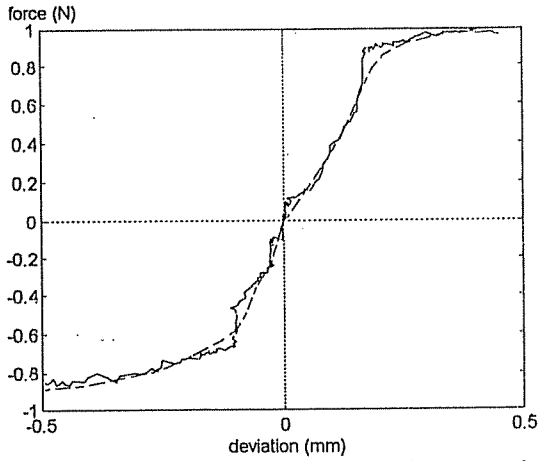

Figure 15 Stiffness characteristic of the proportional actuator around a reference position of 5mm.

5. Conclusion

This paper proposes a method of converting a normal switching solenoid to work as a proportional actuator. The control characteristics of the solenoid is investigated and a nonlinear control model is obtained. Then, an intelligent control strategy based on dual rate cascade control and force compensation is proposed. This control method is implemented on a typical industrial solenoid valve. Both computer simulation and hardware implementation confirm that the solenoid can be controlled with reasonably good accuracy. However it is best to avoid travelling into the two end limits, because of hysteresis and limited force range.

The proposed method is simple, easy to implement, and the control algorithm can easily be transported to a low cost processor.

6. References

[1] N.C. Cheung, M.F. Rahman, K.W. Lim, "Simulations and experimental studies towards the development of a proportional solenoid", Australian Universities Power Engineering Conference, Vol. 2, pp 582-587, Sept 1993, Australia.

[2] T.J.E. Miller, "Switched reluctance motor drives", Ventura, CA: Intertec Communications, 1988.

[3] N.C. Cheung, K.W. Lim, M.F. Rahman, "Modelling a linear and limited travel solenoid", IEEE Proceedings on Industrial Electronics Society annual general meeting, IECON'93, Vol.3, Nov 1993.

[4] D.A. Torrey, J.H. Lang, "Modelling a non linear variable reluctance motor drive", IEE Proceedings, Vol. 137, pt. B, no. 5, pp 314-326, Sept 1990.

[5] D.G. Manzer, M. Varghese, J.S. Throp, "Variable reluctance motor characterization", IEEE Transactions on Industrial Electronics, Vol. 36, no. 1, pp 56-63, Feb 1989.

[6] A.E. Fitzgerald, "Electric machinery: the processes, the devices, and systems of electro-mechanical energy conversion", McGraw Hill, 1971.

[7] A. Isidori, "Nonlinear control systems, an introduction", 2nd edition, New York: Springer-Verlag, 1989.

[8] M. Illic-Spong, R. Marino, S.M. Peresada, D.G. Taylor, "Feedback linearizing control of switched reluctance motors", IEEE Transactions on Automatic Control, Vol. AC-32, no. 5, pp 371-379, 1987.

[9] D.G. Taylor, "An experimental study on composite control of switched reluctance motors", IEEE Control Systems Magazine, Vol. 11, iss. 6, pp 31-36, Feb 1991.

[10] J.M. Stephenson, J. Corda, "Computation of torque and current in doubly salient reluctance motors from non linear magnetisation data", IEE Proceedings, pt. B, vol 126, pp 393-396, 1979.

[11] R. Krishnan and P. Materu "Measurement and instrumentation of a switched reluctance motor," IEEE Industry Applications Society annual meeting, 1989, vol. 1, pp 116-121.

[12] A. Ferro and A. Raciti, "A digital method for the determination of magnetic characteristics of variable reluctance motors," IEEE Trans. on Instrumentation and Measurement, vol. 39, no. 4, pp 604-608, Aug 1990.